

Resistance hysteresis in the integer and fractional quantum Hall regime

E. Peraticos^{1,2,*}, S. Kumar^{1,†}, M. Pepper^{1,2}, A. Siddiki^{3,4}, I. Farrer⁵, D. Ritchie⁶, G. Jones⁶ and J. Griffiths⁶

¹Department of Electronic and Electrical Engineering, University College London, Torrington Place, London WC1E 7JE, United Kingdom


²London Centre for Nanotechnology, 17-19 Gordon Street, London WC1H 0AH, United Kingdom

³Paul-Drude-Institut für Festkörperelektronik, Leibniz-Institut im Forschungsverbund Berlin e.V., Hausvogteiplatz 5-7, 10117 Berlin, Germany

⁴Ekendiz Tanay Center for Arts and Science, Department of Physics, Ula, Muğla 48650, Turkey

⁵Department of Electronic and Electrical Engineering, The University of Sheffield, Sheffield, S10 2TN, United Kingdom

⁶Cavendish Laboratory, JJ Thomson Avenue, Cambridge, CB3 0HE, United Kingdom

 (Received 6 December 2022; revised 23 March 2023; accepted 15 May 2023; published 30 May 2023)

We present experimental results where hysteresis is observed depending on the magnetic field sweep direction in the integer quantum Hall regime of a high-mobility two-dimensional electron system formed in a GaAs/AlGaAs heterostructure. We analyze the results based on the screening theory and show that the anomalous effects observed stem from the nonequilibrium processes resulting from the formation of metal-like and insulator-like regions due to direct Coulomb interactions and the dissipative nature of the Hall bar together with the scattering-influenced contacts. Furthermore, the hysteretic behavior is shown for the integer filling factors $\nu = 1, 2$, and 4 and for certain fractional states at the longitudinal resistance. We argue that the nonequilibration is not only due to contacts, in contrast, but also due to the nature of the finite size dissipative Hall bar under interactions and Landau quantization.

DOI: [10.1103/PhysRevB.107.205307](https://doi.org/10.1103/PhysRevB.107.205307)

I. INTRODUCTION

The hysteresis phenomena have been intensively studied and usually attributed to nonequilibrium ferromagnetic materials related to the spin polarization of the nucleus or the charge carriers. A similar ferromagnetic hysteresis has also been observed in the integer and fractional Hall systems [1–9] realized using low-dimensional electron systems. One of the most exciting charge carrier systems is the two-dimensional electron system (2DES), which three Nobel Physics prizes have praised, including the ordinary 2DES induced at 3D heterostructures yielding the integer and fractional quantum Hall effects (IQHE/FQHE) [10,11] and solely 2D materials such as graphene [12]. These phenomena have been discussed and studied within the context of various theoretical frameworks like dynamic nuclear polarization (DNP) [8,9], presence of spin-glass [6], quantum Hall ferromagnets [2–4,6], the presence of nonequilibrium currents (NECs) [1,5,13] among others which take into account the formation of compressible (metal-like) and incompressible (insulator-like) strips [7,14]. In the cases mentioned above, hysteresis flows either clockwise or anticlockwise, depending on the quantum state. Whereas in conventional ferromagnets, hysteresis flows in an anticlockwise direction.

In this paper, the hysteretic behavior is discussed within the screening theory of the quantum Hall effect. On the one hand, the well-appreciated and utilized gauge-invariant theories [15–17] assume adiabaticity in charge transport. However, the magnetic field (B) sweep direction dependency is a nonequilibrium phenomenon and can not be handled within the frame of adiabaticity. On the other hand, the theories which take into account the finite size effects, such as physical boundaries, yield Landauer-Büttiker type edge picture [18]. Here, the 2DES is assumed to be dissipationless and the equilibration processes occur at the contacts. This picture cannot describe nonequilibrium processes taking place at the dissipative Hall bars. In contrast with the local probe experiments [19–21], Landauer-Büttiker edge states are coupled to the source-drain and probe contacts without scattering. Hence, the edge-state picture explains the observed hysteresis via the non-Ohmic behavior of the contacts due to impurities influencing the transport. However, the sweep direction-dependent observations lack a clear description once the current amplitude exceeds the linear response regime, [22,23] where the imposed current affects the formation of the edge reconstruction, particularly at the fractional quantum Hall effect regime [24,25].

This nonlinearity reflects itself in B sweep direction and equilibration processes. Here we investigate the observed hysteresis within the nonlinear and nonequilibrium frame of screening theory. This theory stems its rationale from the vital link between the momentum q and frequency ω dependent dielectric function $\epsilon(q, \omega)$ and the density of states (DOS, $D(E)$). Namely one considers a time-independent, i.e., $\omega \rightarrow 0$, external potential $V_{\text{Ext}}(q)$ and the screened potential $V_{\text{Scr}}(q)$ is given by

$$V_{\text{Scr}}(q) = \frac{V_{\text{Ext}}(q)}{\epsilon(q)}, \quad (1)$$

*Currently at School of Physical and Mathematical Sciences, Nanyang Technological University, 21 Nanyang Link, 637371, Singapore.

†sanjeev.kumar@ucl.ac.uk

Published by the American Physical Society under the terms of the [Creative Commons Attribution 4.0 International](https://creativecommons.org/licenses/by/4.0/) license. Further distribution of this work must maintain attribution to the author(s) and the published article's title, journal citation, and DOI.

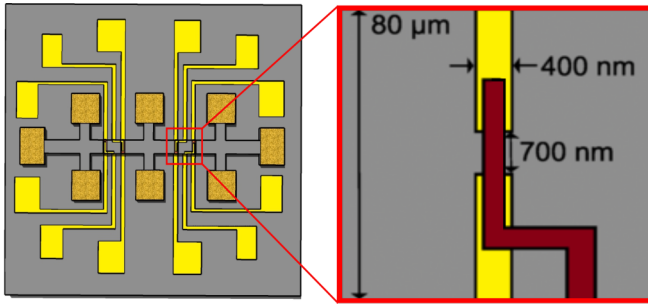


FIG. 1. The device geometry is shown with the figure on the left showing the whole Hall bar structure with the dark yellow rectangles being the Ohmic contacts. The bright yellow structures are titanium/gold optical gates used as contacts with the split gates and top gates, shown in a zoomed-in figure on the right. The Hall bar has a width of $W_H = 80 \mu\text{m}$, and the length is $L_H = 1800 \mu\text{m}$. The split gates (shown in yellow) are 700 nm apart and have a width of 400 nm . The top gate (dark brown) is separated from the split gates via PMMA.

where $\epsilon(q) = 1 + \frac{2\pi e^2 D(E)}{\kappa|q|}$ is explicitly dependent on DOS and κ (~ 12.4 for GaAs) is the dielectric constant of the heterostructure. Hence the quantization emerging from the magnetic field inevitably alternates the screening properties of the 2DES from linear (without magnetic field) to strongly non-linear [7,26–29]. Investigating the observed hysteresis within the screening theory framework improves our understanding of the formation of incompressible strips (ISs) and their link to spin-related phenomena. It is crucial to emphasize that screening theory can handle both the contacts, disorder and nonequilibrium phenomena up to a reliable extent [7,22,30].

II. SAMPLE AND METHODS

In the present work, we performed magnetotransport measurements on a GaAs/Al_{0.33}Ga_{0.67}As heterostructure grown by molecular beam epitaxy. The two-dimensional electron system (2DES) is formed at the GaAs/AlGaAs interface at approximately 100 nm from the surface of the heterostructure. The electron carrier density was calculated in the dark (light) to be $n_0 = 1.6 \times 10^{11} \text{ cm}^{-2}$ ($4.45 \times 10^{11} \text{ cm}^{-2}$) and its mobility of $\mu_e = 0.37 \times 10^6 \text{ cm}^2 \text{ V}^{-1} \text{ s}^{-1}$ ($1.05 \times 10^6 \text{ cm}^2 \text{ V}^{-1} \text{ s}^{-1}$). The purpose of controlled illumination was to tune carrier concentration and mobility of 2DES, and suppress the possibility of parallel conduction by photoexcited low-mobility carriers [31]. The Hall bar formed on the heterostructure has split gates and a top gate fabricated using lithographic methods. The split-gates are isolated from the top gate via a thin poly (methyl methacrylate) (PMMA) layer. Their widths are 400 nm , and the gap between the split gates is 700 nm , as seen in Fig. 1. The width of the Hall bar is $80 \mu\text{m}$, and a length of $1800 \mu\text{m}$. The contacts used to measure the Hall resistance, R_{xy} , are separated by $300 \mu\text{m}$, whereas the contacts used to measure longitudinal resistance R_{xx} are $1080 \mu\text{m}$ apart. As for the split-gate used for the data presented in this paper, it is located $230 \mu\text{m}$ from the left R_{xx} contact and $850 \mu\text{m}$ from the right R_{xx} contact. In addition, the split-gate voltages V_{sg} used for the measurements are given in Fig. 1 in Ref. [25].

When the top gate was not used, it was left floating in these measurements.

All measurements were performed at 10 mK , unless stated otherwise, within a dilution refrigerator. We use the four-terminal lock-in amplifier method to measure the longitudinal and transverse resistance. The excitation current was set to 10 nA at 77 Hz unless otherwise stated.

III. THE MODEL

The quantum Hall effect has been the subject of experimental and theoretical studies in many fields, not only as a means of standardizing resistance units [32]. The effects are also rich in spin-related properties, such as the ferromagnetic spin ordering [2–4,6], spin transitions at the FQHE [4,33,34] and skyrmionic spin excitations [35,36]. These experiments present the hysteretic-like behavior at the longitudinal magnetoresistance. However, their origin is still disputed and not well understood. For hyperfine interactions, the relaxation time is assumed to be approximately $\tau \geq 25 \text{ s}$, and the spin-orbit interactions are considered the primary cause [8]. On the other hand, the Ising model is considered to be the origin of the observed phenomena, e.g., spin-glass [6] and quantum Hall ferromagnet behavior [2,4]. Since all the theories rely on the bulk picture of the QHEs and spin polarization, they are somewhat challenged at finite size samples where unpolarized states like $\nu = 2$ and 4 also show hysteresis. Similar to the bulk or localization picture of the QHE, these theories consider an unbounded system or periodic boundary conditions, which can not be justified in our experiments. Therefore finite-size effects and direct Coulomb interactions should be included. However, the indirect Coulomb interactions, i.e. exchange and correlation, may enhance spin-orbit coupling. Hence, a detailed theory is valuable in uncovering the hysteresis effect observed and reported here.

This section introduces the mainframe of the screening theory [26–29] and discusses our results within this frame as a possible origin of the hysteresis observed. A very similar hysteresis observed in a bilayer electron system is well explained by this model, which also takes into account nonequilibrium processes due to the formation of metal-like compressible and insulator-like incompressible strips (CSs and ISs, respectively) [7]. The model predicts a clear link between the existence of ISs and the overshoot effect and is shown explicitly in Refs. [25,37]. It was shown that the “well-developed” ISs form at the plateau regime, and the position of the ISs and the potential distribution change depend on the magnetic field strength B . By “well-developed,” we mean that the widths of the ISs (W_{IS}) are more extensive than the thermodynamical length scales, such as the Fermi wavelength (λ_F) and quantum mechanical length scales like the magnetic length (ℓ_B). In this regime, the insulator-like incompressible strips can decouple the Hall probe contacts, and the resistance is quantized [29]. However, once the widths of the ISs become narrower than the Fermi wavelength, either due to thermal activation or driven by the electrical force resulting from the Hall potential gradient, it is possible to scatter electrons across these strips. Hence the Hall resistance quantization is smeared out, and the longitudinal resistance no longer approaches zero at finite temperatures. Such underdeveloped ISs manifest themselves,

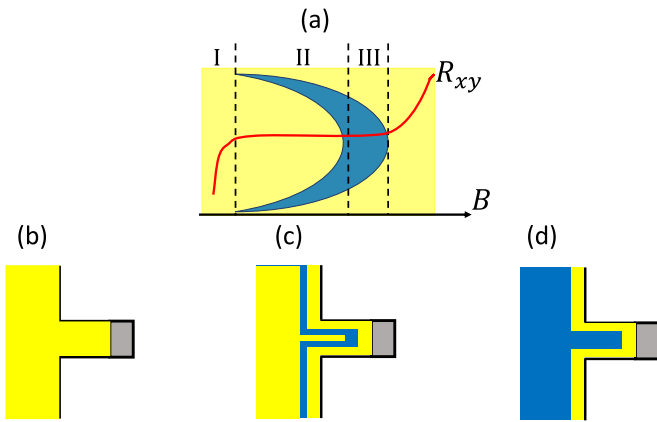


FIG. 2. (a) The positions and the widths of the incompressible (dark, blue) and compressible (light, yellow) regions together with the Hall resistance [solid (red) line] as a function of the magnetic field, B . (b) The illustration of the compressible [light (yellow) region] regions and probe contact (grey, dark) for magnetic field interval I. (c) The quantized Hall plateau is observed since an incompressible stripe at the edge decouples the rest of the sample from the probe contact, interval II. (d) At the plateau's high magnetic field edge, the entire bulk becomes incompressible, interval III.

together with the inter-Landau-level scattering, as resistance overshoot at the Hall resistance [25,37]. A similar scattering process occurs when one considers the longitudinal resistance, as hysteresis. In the case of longitudinal resistance anomaly, namely, hysteresis, the sweep direction plays a key role. In early experimental investigations of the equilibrium processes regarding the ISs, the equilibration time scales are measured to be as long as 24 hours [14]. Hence, the equilibration time scales of the ISs are much longer than the time scales of the magnetic field sweep rate. Given the long relaxation time scale, one can reliably consider the system in hand to be Markovian (history-dependent). Therefore one should consider the system's previous state to understand the data [7]. Also, this long timescale indicates that neither the DNP nor the electron spin polarization can account for the observed hysteresis reported here.

The essential field sweep direction dependency of the measured resistance can be understood in forming the incompressible regions (depicted by (light, yellow) within the sample. In contrast, the compressible regions are depicted in the dark (blue), Fig. 2. Understanding the evolution of the incompressible strips as a function of magnetic field and sweep direction is essential. We start from the low magnetic field side of a plateau: First, the 2DES is at a complete compressible state where electron screening is nearly perfect, the region I in Fig. 2(a) corresponding to the case of compressibility is demonstrated in Fig. 2(b). Hence the potential distribution at the bulk of the sample is flat due to the entire compressibility of the 2DES, resulting in a metal-like good screening. The grey regions depict the metallic probe contacts in Fig. 2. The contacts are in equilibrium with the 2DES, i.e., electrically and thermodynamically. Hence the system is in equilibrium, and hysteresis is expected.

The bulk becomes incompressible at higher fields of an ideal (potential fluctuation-free) sample. In contrast, the edges

are compressible, as shown in Fig. 2, i.e., region III and illustrated in Fig. 2(d). The scheme mentioned above is the typical behavior observed by local probe experiments [20,21], and predicted by the screening theory calculations [25,29,38]. The lower part of Fig. 2 demonstrates the coupling of the probe contacts (grey region) to the compressible [light (yellow) region] and incompressible (dark, blue, region) regions. In all cases, the probe contacts are in equilibrium with the compressible region in their close vicinity. However, in regions II and III, the incompressible edge strips (II) or bulk (III) decouple the contacts from the inner regions from the transverse (Hall) probe contacts. As shown in our previous work, this results in an overshoot effect [25].

Here, we utilize the screening theory considering the anomaly (the observed hysteresis) in the longitudinal resistance and, in comparison, approaching the Hall plateau from low B . Hence, equilibration can take place quickly. Furthermore, an increase in B results in narrow ISs barely decoupling the probe contacts. In contrast, while approaching the same part of the Hall plateau from higher fields, there already exists a well-developed ISs at the edges, which essentially decouples the probe contacts fairly well, preventing equilibration processes. By this qualitative discussion, we can explain the following consistently: (1) no hysteresis behavior can be observed at the low field edge of the Hall plateau and (2) the hysteresis can not be observed at the very high field of the plateau. More importantly, the observed hysteresis is related to the equilibration processes through the ISs, which depend on their widths.

IV. RESULTS AND DISCUSSION

In this section, we present our experimental observations and discuss them in the frame of the close relationship between the overshoot effect [25,37] and the magnetoresistance hysteresis. It is important to recall that the well-developed incompressible strips [i.e., $W_{IS} > \lambda_F > \ell_B$] presume zero resistance in the longitudinal direction at zero temperature since scattering is suppressed due to vanishing density of states (DOS) at the Fermi energy. On the other hand, these incompressible strips decouple transverse contacts due to their high quantum capacitive properties, again due to the vanishing DOS at the Fermi level. Here, we first show the strong correlation between the overshoot effect [Fig. 3(a)] and the longitudinal resistance measurements with resistance hysteresis noticed while varying the magnetic field B , Fig. 3(b). It should be noted that although illuminating the sample can induce parallel conduction [31], and it could be thought that the nonvanishing R_{xx} is a consequence of this. However, the fact that R_{xy} does not deviate from its quantized values, as in our case, the contribution from parallel conduction may be ruled out. As the constrictions are narrow in this device, it is thought that inter Landau scattering takes place at the longitudinal transport, whereas Hall probes are well decoupled from each other yielding a well-developed Hall resistance quantization. Additionally, as discussed in Ref. [25], the absence of $\nu = 3$ is due to the fact that the evanescent regimes of the incompressible strips overlap and therefore the overshooting effect takes place whereas for the $\nu = 5$ and 7, the incompressible strips do not overlap with the evanescent regime over other

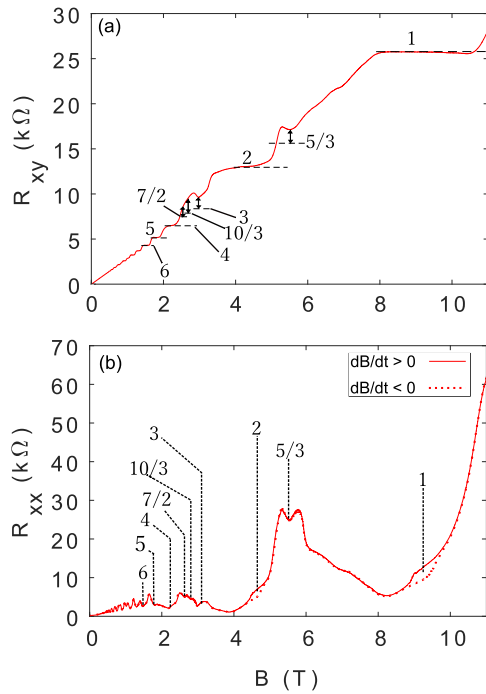


FIG. 3. (a) R_{xy} vs B where the two-way arrows indicate the transverse resistance anomalies for the corresponding integral and fractional states. (b) R_{xx} vs B where the black dashed lines indicate the corresponding location of the ISs for the integral and fractional states. The solid red trace is the R_{xx} measured for an increasing B ($dB/dt = +6$ T/h) and the red dashed trace is the R_{xx} measured for decreasing B ($dB/dt = -6$ T/h). The mismatch between the two traces creates noticeable hysteretic features at $\nu = 1$ and 2. The numbers indicated are the corresponding filling factors. $V_{sg} = V_{fg} = 0$ V.

strips, therefore, no overshooting occurs for these plateaus. In Fig. 4, the hysteresis is noticed predominately for the integer $\nu = 1, 2$, and 4, see insets of Fig. 4. However, we also observe a hysteretic behavior for a fractional state, in inset (a). The hysteresis follows a clockwise direction and is at the center around the B values, using the self-consistent screening theory described in Ref. [25]. The vertical black dashed lines focus on B intervals at the insets of Fig. 4. Moreover, in the considered B intervals, the hysteretic behavior presents the most prominent part of the loop corresponding to the area of the widest ISs for the ν related to it. In inset (a) of Fig. 4 an anticlockwise loop also appears. This hysteretic loop, however, seems to be centered around a B value where a fractional filling factor, ν_f , would be expected, although no minimum point in R_{xx} appears. Furthermore, by increasing the operating temperature, T and the bias current, I , more hysteresis loops that correspond to fractional states appear, with varying loop directions.

Specifically, in Figs. 5 and 6, we show the arrow directions. We observe that some of these loops start with an anticlockwise/clockwise direction but then change to clockwise/anticlockwise loops as T increases until they eventually smear out. Similarly, for the integer ν , the loops smear out with increasing T , but they retain their clockwise loop direction until they disappear. The clockwise flow of the hys-

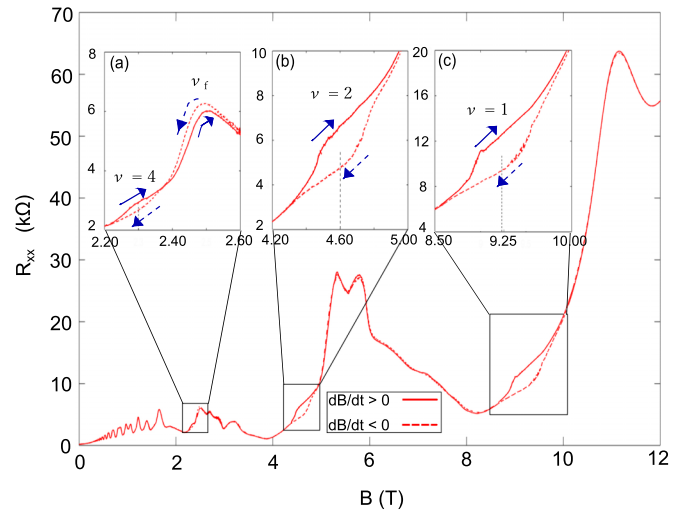


FIG. 4. R_{xx} vs B where the solid red trace is the R_{xx} measured for an increasing B ($dB/dt = +6$ T/h) and the red dashed trace is the R_{xx} measured for decreasing B ($dB/dt = -6$ T/h). The mismatch between the two traces creates noticeable hysteretic features at $\nu = 1, 2$, and 4. The black dashed lines indicate the corresponding location of the ISs for the integral and fractional states, aligning with the hysteretic feature. Insets (a)–(c) show the zoomed-in parts of the traces where we observed hysteresis. $V_{sg} = V_{fg} = 0$ V.

teresis for the integer ν is in agreement with data obtained in Refs. [1,2,7,8]. As for the varied presence of clockwise and anticlockwise flowing hysteresis for fractional valued ν , this also seems to agree with Refs. [3,4,6,8]. In addition, we note that the hysteretic areas decrease in size from $\nu = 1$ to $\nu = 4$ following the decrease of the width of the ISs [25].

Remarkably we observe that the shape of the hysteresis alters as the temperature increases and extends to higher magnetic fields, as presented in Fig. 6 for both $\nu = 2$ and 4. Such alteration could be due to the ISs breakdown and there-

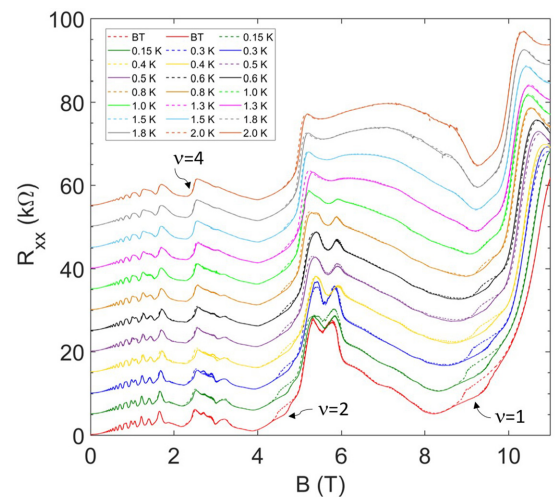


FIG. 5. The variation of R_{xx} vs B , where the hysteretic features for $\nu = 1, 2$, and 4 are shown for different temperatures from BT to 2 K. The solid color traces are for increasing B ($dB/dt = +6$ T/h) and the dashed color traces are for decreasing B ($dB/dt = -6$ T/h). The traces were offset vertically for clarity by $+5$ $k\Omega$. $V_{sg} = V_{fg} = 0$ V.

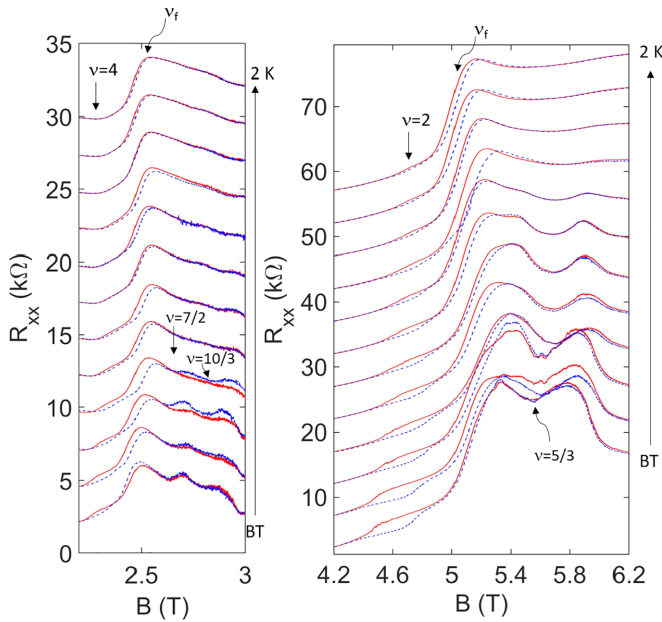


FIG. 6. R_{xx} vs B , where the zoomed-in temperature dependence of the hysteretic features for $\nu = 4$ and 2 are shown in the left and right plots, respectively. The solid color traces are for increasing B ($dB/dt = +6$ T/h) and the dashed color traces are for decreasing B ($dB/dt = -6$ T/h). The traces for the left diagram were offset vertically for clarity by $+2.5$ k Ω and the one on the right by $+5$ k Ω . $V_{sg} = V_{tg} = 0$ V.

fore entering an evanescent regime, namely $\lambda_F > W_{IS} > \ell_B$. Hence, the current is leaking between the ISs and therefore altering the system's current distribution profile. As a direct consequence, scattering effects are enhanced. Furthermore, notice that for $\nu = 3$, we do not observe hysteresis. The fact that multiple evanescent ISs are overlapping explains the nonobservation of the hysteresis at this particular ν as opposed to $\nu = 1, 2$, and 4 , see Ref. [25]. This approach also explains the phenomenon we observe only for these ν , since they are the widest of all the ISs, especially for $\nu = 1$ and 2 and to a lesser extent for $\nu = 4$ as it is barely visible on a larger scale.

We performed a set of measurements where we kept the temperature of the system constant at BT (~ 10 mK) and varied the bias current from 10 to 4550 nA, as shown in Fig. 7. We noticed an interesting behavior for increasing current values as opposed to the temperature measurements, the hysteretic behavior for $\nu = 1$ extends to higher B values, however for $\nu = 2$ and 4 , the opposite occurs, that is the hysteretic loop becomes clearly defined as a closed-loop, see Fig. 7. As seen from Fig. 7(b), the plateau regarding $\nu = 1$ is also the first plateau to breakdown as opposed to the $\nu = 2$ and 4 , which become well defined with increasing current similar to the fractional ISs breakdown. Therefore no overlapping of evanescent ISs takes place. Additionally, as the current increases for $\nu = 1$, a large tilt in the potential landscape takes place, leading to an increase in the size of the hysteresis and leading to a "breakdown regime," see traces for $I = 640$ to 1200 nA, where the hysteresis alters its shape. At 2140 nA, the local temperature of the electron gas increases significantly, stemming from the current leakage (via Joule heating)

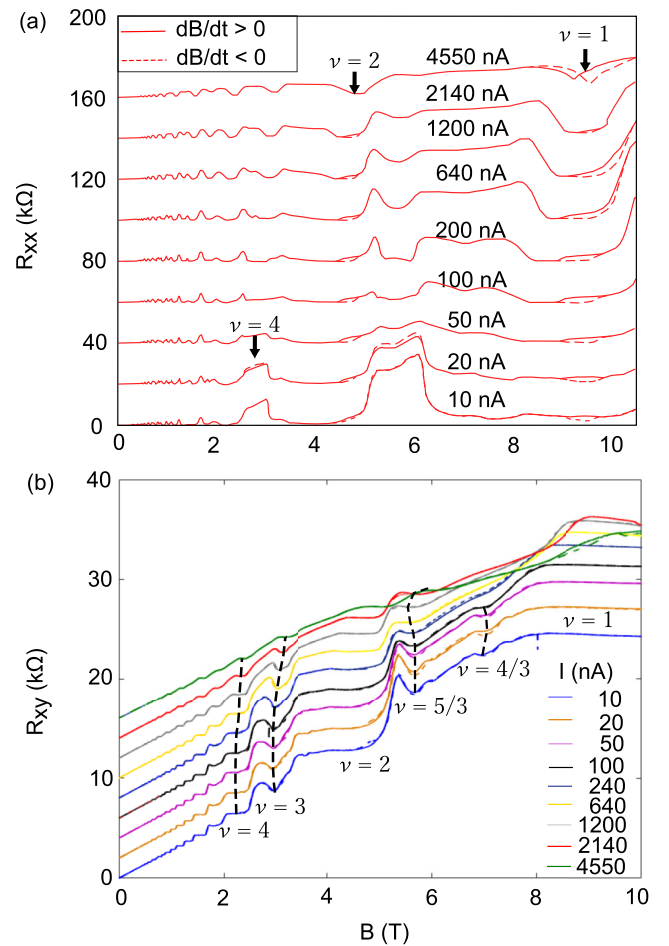


FIG. 7. (a) R_{xx} vs B , where the hysteretic features for $\nu = 1, 2$, and 4 are shown for different bias currents at constant BT. The solid red colored traces are for increasing B ($dB/dt = +6$ T/h) and the dashed color traces are for decreasing B ($dB/dt = -6$ T/h). The traces were offset for clarity by $+20$ k Ω . (b) The plot of R_{xy} vs B for different sample currents. The dashed black lines show the evolution of the stated ν . $dB/dt = \pm 6$ T/h and offsetted by $+2$ k Ω . $V_{sg} = V_{tg} = 0$ V.

that occurs while ISs are entering the evanescent regime and leading to the significantly diminishing hysteresis in size and is at a fragile state. Similarly, in a less notable manner, this occurs for both $\nu = 2$ and 4 , where the hysteresis increases with increasing current but then starts to weaken due to local heating. Eventually, for $I = 4550$ nA, the hysteretic loops for $\nu = 2$ and 4 disappear. For $\nu = 1$, though, there seems to be an anomalous form of hysteresis forming as we further increase the current to 4550 nA. The anomalous form occurs only for $\nu = 1$, which could be due to excessive current causing asymmetry in the system and thus the breakdown of the QHE.

Furthermore, in an additional measurement, we applied split gate voltage, V_{sg} and investigated the hysteresis pattern and varied V_{sg} from 0 to -2.81 V, which is close to the pinch-off value of the quasi-1D channel [25]. The current and the temperature were constant at $I = 10$ nA and BT, respectively. As can be noticed in Fig. 8, the area of the hysteretic loops increases exponentially as the 1D channel is more con-

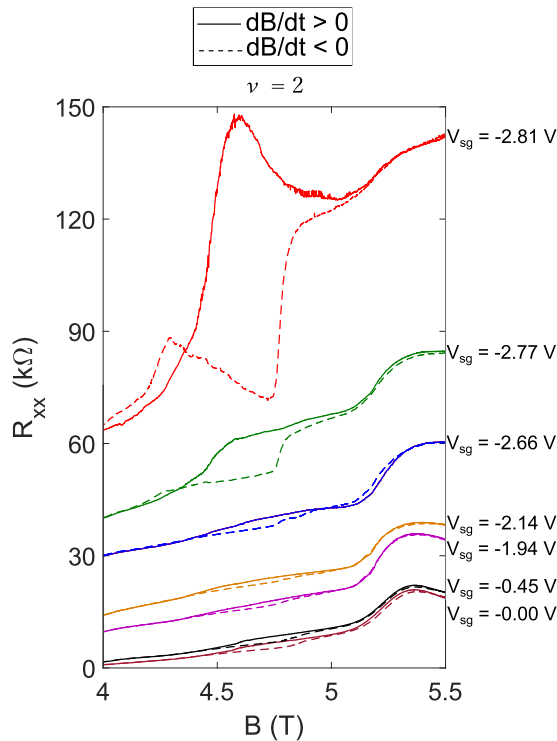


FIG. 8. R_{xx} vs B , where the hysteretic features for $\nu = 2$ are shown for different V_{sg} at constant BT and $I = 10$ nA. The solid color traces are for increasing B ($dB/dt = +6$ T/h) and the dashed color traces are for decreasing B ($dB/dt = -6$ T/h). $V_{tg} = 0$ V.

stricted, or strongly confined. It should be noted that although the split gate voltage changes, the position of the hysteresis points does not change. This may be due to the fact that their location depends on the 2DEG density, and perhaps not on the 1D constriction width. However, the density of electrons within the constriction does affect the incompressible strips; with negatively increasing split-gate voltage the incompressible strips are being forced closer together thus increasing the hysteretic behavior. Similarly, we observe an enhancement in the hysteretic area while keeping the V_{sg} constant at -2.12 V and by varying the V_{tg} from 0 to -0.70 V for $\nu = 1$ and 2 (Fig. 9). We think that the enhanced hysteresis by negatively increasing V_{sg} and V_{tg} could arise from the scattering effects as discussed in the literature [1,5,9].

A seemingly recent theory using incompressible and compressible states by Budantsev *et al.* [1] is following the screening theory and explains the data presented in this paper. This theory proposes that as the magnetic field is varied, an azimuthal electric field is induced in the system, causing a radial current density between the edges of the sample and the center [1]. This mechanism, in turn, creates a radial electric field, driving nonequilibrium currents (NECs). The constrictions, though defined in Ref. [1] were achieved lithographically rather than with electrostatic methods. However, the effects are translational. Therefore, for $dB/dt > 0$, the electric field vortex creates an electron outflow from the edge to the bulk, decreasing the area occupied by the incompressible strip and the ISs retreat from the edge of the mesa. Consequently, as the barrier height of the constriction increases by negatively

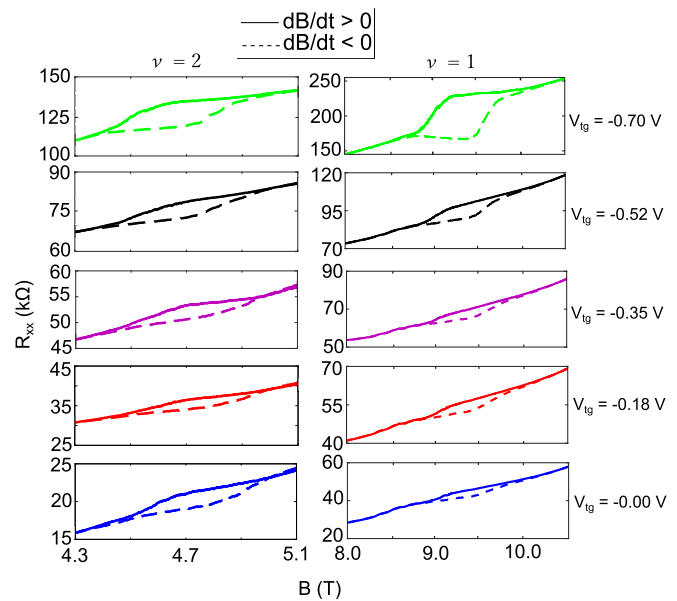


FIG. 9. R_{xx} vs B , at fixed $V_{sg} = -2.12$ V and varying the V_{tg} from 0.00 V to -0.70 V. The left-hand side shows the evolution for $\nu = 2$ and the right one for $\nu = 1$. The solid color traces are for increasing B ($dB/dt = +6$ T/h) and the dashed color traces are for decreasing B ($dB/dt = -6$ T/h).

increasing V_{sg} , the opposite edge channels are brought closer together, leading to a higher backscattering and finally an increase in resistance which is also noticed in our results [1]. When $dB/dt < 0$, the electric field formed drives electrons from the bulk into the sample edges, resulting in the incompressible strips occupying more space and shifting closer to the mesa edges. Therefore the opposite edge currents move further away from each other compared to the equilibrium state which reduces the backscattering taking place and so the resistance is suppressed [1].

The mechanism for the clockwise direction of the hysteresis is a consequence of the rapid movement of the ISs positions as well as intense backscattering taking place with $dB/dt > 0$ [1]. Taking into account the suppression of backscattering due to the well-developed ISs, Siddiki *et al.* [7] elaborate that the presence of ISs makes it difficult for the system to follow rapid changes in the potential distribution and the ISs positions as current-carrying edge states are not in direct equilibration with the Ohmic contacts. A slight change in B results in a rapid change in the potential distribution. However, the screening response of electrons is retarded (due to their poor screening properties at an IS), manifesting as the hysteretic effect. This mechanism would also explain why we see the hysteretic loop centered on the B values, which correspond to the position at which the IS has the largest thickness. In addition, this could illustrate why the hysteresis is almost at its widest part at these B values. Additionally this explains why the hysteresis is larger for $\nu = 1$ than $\nu = 2$ and $\nu = 4$ in that order.

However, it is still unclear why the fractional states seem to have anticlockwise and clockwise behavior in their hysteresis. A possible explanation was provided by Wald *et al.* [9], suggesting that the clockwise behavior is due to spin-flip

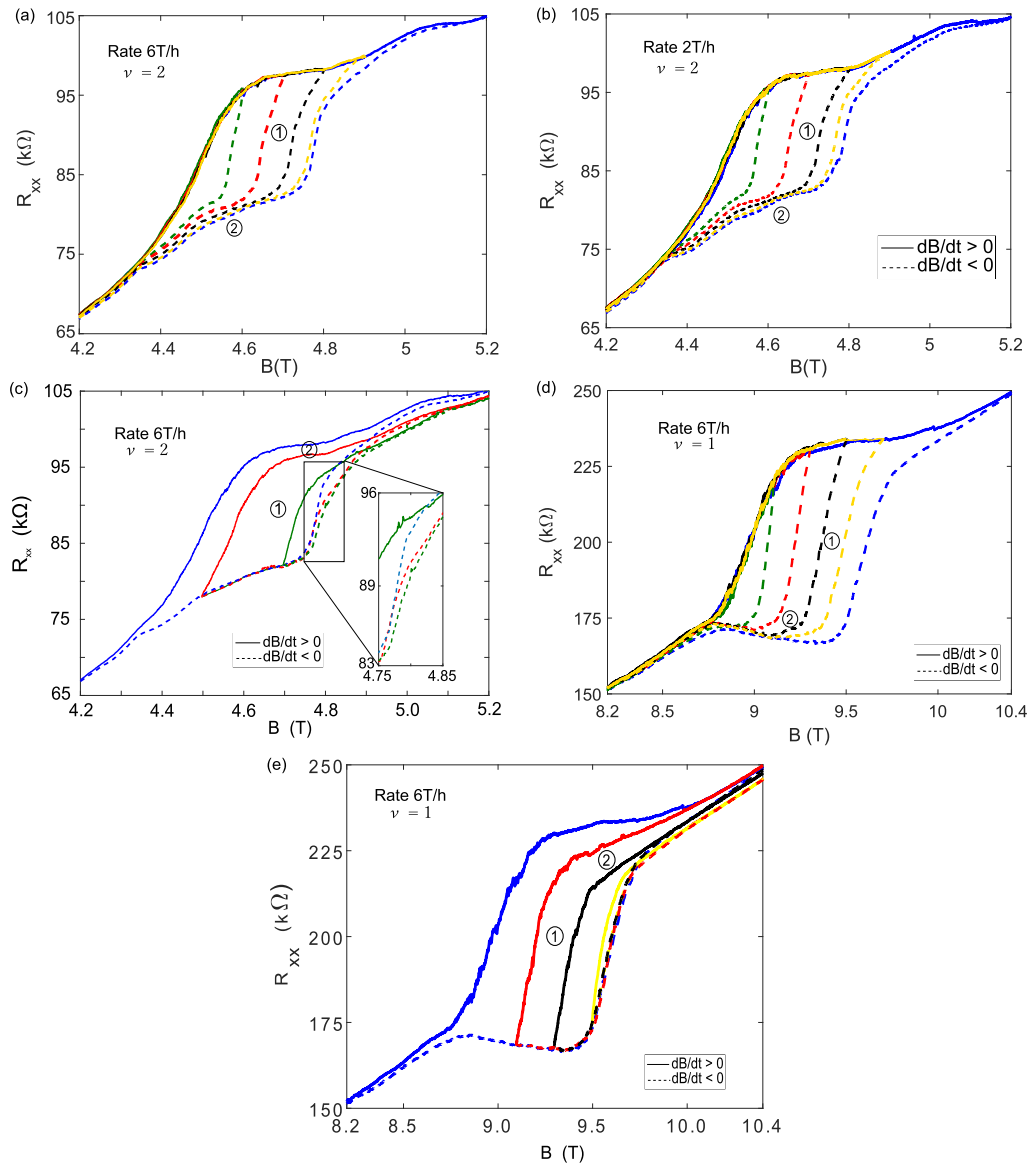


FIG. 10. Minor hysteresis loops enveloped by the main hysteresis loop achieved when measuring R_{xx} vs B [(a)–(c)] for $\nu=2$ and [(d) and (e)] for $\nu=1$. All plots were measured at a rate of $dB/dt = \pm 6$ T/h except for (b) at ± 2 T/h. For (a), (b), and (d), the minor loops are formed by increasing B to a fixed B , and then decreasing B to form a minor loop, and for (c) and (e), the minor loops are formed by decreasing B first and then increasing it to form a minor loop. $V_{sg} = -2.12$ V and $V_{sg} = -0.70$ V.

backscattering, and the opposite behavior is due to spin-flip forward scattering. However, the limitation with this explanation is that it only works if there is a quantum point contact, QPC, which causes scattering effects. In our case, these behaviors are noticed for the fractional states even when no constriction is present, as is for the case of the temperature and current dependence measurements in Figs. 5–7. The presence of overlapping evanescent ISs from the fractional and integral ν could be a possible reason behind this. Therefore, with the T increasing, the leakage increases, and therefore we notice that the clockwise hysteresis supersedes the anticlockwise behavior due to one type of scattering occurring more abundantly than the other between the ISs.

Another measurement was conducted by pausing B while being on the hysteresis curve and then sweeping B in opposite direction as can be seen in Fig. 10. In the case of Figs. 10(a),

10(b) and 10(d), minor concurrent loops within the main hysteresis loop were formed by stopping the forward sweeping B , say at 4.6 T, reversing the B sweep direction, forming the dotted-green curve, and then stopping B at the initial point of hysteresis curve at 4.2 T. This process is repeated, and the next minor loop in dotted-red curve is formed when the forward B sweep was interrupted at around 4.7 T. For the cases of Figs. 10(c) and 10(e) the opposite occurred, the minor loops were formed while B sweep was decreasing along the reverse section of the hysteresis loop. In both cases, we notice that there are two regimes, ① and ②. On the change of B , that is from increasing/decreasing to decreasing/increasing, the system seems to enter a phase where the R_{xx} values change rapidly, as in ①, but the system then seems to enter a slow R_{xx} changing phase, indicated by ②. This phase change was also studied for various dB/dt rates of ± 6 T/h and

± 2 T/h, as seen in Fig. 10, though without any noticeable change.

V. CONCLUSION

We investigated the anomalous hysteretic behavior in the longitudinal magnetoresistance of the 2DES formed in a GaAs/AlGaAs heterostructure. We analyze the results based on the screening theory and show that the anomalous effects appear from the nonequilibrium processes resulting from the formation of compressible and incompressible strips within the 2DES and the dissipative nature of the Hall bar. Our results

give further insight into the observation of nonequilibrium phenomena, in particular, the anomalous magnetoresistance hysteresis at certain integer as well as fractional filling factors, which we hope will generate further interest in the field.

ACKNOWLEDGMENTS

The work was funded by the Engineering and Physical Sciences Research Council (EPSRC), United Kingdom Research and Innovation (UKRI), UK, and the UKRI Future Leaders Fellowship (Ref. No. MR/S015728/1). A.S. was funded by Tübitak Project #2219.

-
- [1] M. Budantsev, D. Pokhabov, A. Pogosov, E. Y. Zhdanov, A. Bakarov, and A. Toropov, Hysteretic phenomena in a 2DEG in the quantum Hall effect regime, studied in a transport experiment, *Semiconductors* **48**, 1423 (2014).
 - [2] V. Piazza, V. Pellegrini, F. Beltram, W. Wegscheider, T. Jungwirth, and A. H. MacDonald, First-order phase transitions in a quantum Hall ferromagnet, *Nature (London)* **402**, 638 (1999).
 - [3] H. Cho, J. B. Young, W. Kang, K. L. Campman, A. C. Gossard, M. Bichler, and W. Wegscheider, Hysteresis and Spin Transitions in the Fractional Quantum Hall Effect, *Phys. Rev. Lett.* **81**, 2522 (1998).
 - [4] J. H. Smet, R. Deutschmann, W. Wegscheider, G. Abstreiter, and K. von Klitzing, Ising Ferromagnetism and Domain Morphology in the Fractional Quantum Hall Regime, *Phys. Rev. Lett.* **86**, 2412 (2001).
 - [5] N. Ruhe, G. Stracke, C. Heyn, D. Heitmann, H. Hardtdegen, T. Schäpers, B. Rupperecht, M. A. Wilde, and D. Grundler, Origin and limiting mechanism of induced nonequilibrium currents in gated two-dimensional electron systems, *Phys. Rev. B* **80**, 115336 (2009).
 - [6] J. Eom, H. Cho, W. Kang, K. Campman, A. Gossard, M. Bichler, and W. Wegscheider, Quantum Hall ferromagnetism in a two-dimensional electron system, *Science* **289**, 2320 (2000).
 - [7] A. Siddiki, S. Kraus, and R. R. Gerhardts, Screening model of magnetotransport hysteresis observed in bilayer quantum Hall systems, *Physica E* **34**, 136 (2006).
 - [8] E. V. Deviatov, A. Würtz, A. Lorke, M. Y. Melnikov, V. T. Dolgoplov, D. Reuter, and A. D. Wieck, Two relaxation mechanisms observed in transport between spin-split edge states at high imbalance, *Phys. Rev. B* **69**, 115330 (2004).
 - [9] K. R. Wald, L. P. Kouwenhoven, P. L. McEuen, N. C. van der Vaart, and C. T. Foxon, Local Dynamic Nuclear Polarization Using Quantum Point Contacts, *Phys. Rev. Lett.* **73**, 1011 (1994).
 - [10] K. v. Klitzing, G. Dorda, and M. Pepper, New Method for High-Accuracy Determination of the Fine-Structure Constant Based on Quantized Hall Resistance, *Phys. Rev. Lett.* **45**, 494 (1980).
 - [11] D. C. Tsui, H. L. Stormer, and A. C. Gossard, Two-Dimensional Magnetotransport in the Extreme Quantum Limit, *Phys. Rev. Lett.* **48**, 1559 (1982).
 - [12] C. R. Dean, A. F. Young, P. Cadden-Zimansky, L. Wang, H. Ren, K. Watanabe, T. Taniguchi, P. Kim, J. Hone, and K. Shepard, Multicomponent fractional quantum Hall effect in graphene, *Nat. Phys.* **7**, 693 (2011).
 - [13] A. A. Shevyrin, S. Rathi, P. See, I. Farrer, D. Ritchie, J. Griffiths, G. Jones, and S. Kumar, Nonequilibrium phenomena in bilayer electron systems, *Phys. Rev. B* **107**, L041302 (2023).
 - [14] J. Huels, J. Weis, J. Smet, K. v. Klitzing, and Z. R. Wasilewski, Long time relaxation phenomena of a two-dimensional electron system within integer quantum Hall plateau regimes after magnetic field sweeps, *Phys. Rev. B* **69**, 085319 (2004).
 - [15] R. B. Laughlin, Quantized Hall conductivity in two dimensions, *Phys. Rev. B* **23**, 5632 (1981).
 - [16] D. J. Thouless, M. Kohmoto, M. P. Nightingale, and M. den Nijs, Quantized Hall Conductance in a Two-Dimensional Periodic Potential, *Phys. Rev. Lett.* **49**, 405 (1982).
 - [17] M. Kohmoto, Topological invariant and the quantization of the Hall conductance, *Ann. Phys.* **160**, 343 (1985).
 - [18] M. Büttiker, Four-Terminal Phase-Coherent Conductance, *Phys. Rev. Lett.* **57**, 1761 (1986).
 - [19] P. Weitz, E. Ahlswede, J. Weis, K. Von Klitzing, and K. Eberl, Hall-potential investigations under quantum Hall conditions using scanning force microscopy, *Physica E* **6**, 247 (2000).
 - [20] E. Ahlswede, J. Weis, K. v. Klitzing, and K. Eberl, Hall potential distribution in the quantum Hall regime in the vicinity of a potential probe contact, *Phys. E* **12**, 165 (2002).
 - [21] F. Dahlem, E. Ahlswede, J. Weis, and K. v. Klitzing, Cryogenic scanning force microscopy of quantum Hall samples: Adiabatic transport originating in anisotropic depletion at contact interfaces, *Phys. Rev. B* **82**, 121305(R) (2010).
 - [22] D. Eksi, O. Kilicoglu, O. Goektas, and A. Siddiki, Screening model of metallic nonideal contacts in the integer quantized Hall regime, *Phys. Rev. B* **82**, 165308 (2010).
 - [23] R. R. Gerhardts, K. Panos, and J. Weis, Current-induced asymmetries of incompressible strips in narrow quantum Hall systems, *New J. Phys.* **15**, 073034 (2013).
 - [24] A. Salman, A. I. Mese, M. B. Yucel, and A. Siddiki, Semi-analytical model of Hall resistance anomalies (overshooting) in the fractional quantized Hall effect, *Eur. Phys. J. B* **86**, 203 (2013).
 - [25] E. Peraticos, S. Kumar, M. Pepper, A. Siddiki, I. Farrer, D. Ritchie, G. Jones, and J. Griffiths, Hall resistance anomalies in the integer and fractional quantum Hall regime, *Phys. Rev. B* **102**, 115306 (2020).
 - [26] K. Lier and R. R. Gerhardts, Self-consistent calculations of edge channels in laterally confined two-dimensional electron systems, *Phys. Rev. B* **50**, 7757 (1994).

- [27] J. Oh and R. Gerhardtts, Effects of current and gate voltage on compressible and incompressible strips in a Hall bar, *Physica E* **1**, 108 (1997).
- [28] K. Güven and R. R. Gerhardtts, Self-consistent local equilibrium model for density profile and distribution of dissipative currents in a Hall bar under strong magnetic fields, *Phys. Rev. B* **67**, 115327 (2003).
- [29] A. Siddiki and R. R. Gerhardtts, Incompressible strips in dissipative Hall bars as origin of quantized Hall plateaus, *Phys. Rev. B* **70**, 195335 (2004).
- [30] S. E. Gulebaglan, G. Oylumluoglu, U. Erkaslan, A. Siddiki, and I. Sökmen, The effect of disorder on integer quantized Hall effect, *Phys. E* **44**, 1495 (2012).
- [31] M. Reed, W. Kirk, and P. Kobiela, Investigation of parallel conduction in GaAs/Al_xGa_{1-x}As as modulation-doped structures in the quantum limit, *IEEE J. Quantum Electron.* **22**, 1753 (1986).
- [32] A. Hartland, The quantum Hall effect and resistance standards, *Metrologia* **29**, 175 (1992).
- [33] L. W. Engel, S. W. Hwang, T. Sajoto, D. C. Tsui, and M. Shayegan, Fractional quantum Hall effect at $\nu = 2/3$ and $3/5$ in tilted magnetic fields, *Phys. Rev. B* **45**, 3418 (1992).
- [34] I. V. Kukushkin, K. v. Klitzing, and K. Eberl, Spin Polarization of Composite Fermions: Measurements of the Fermi Energy, *Phys. Rev. Lett.* **82**, 3665 (1999).
- [35] S. L. Sondhi, A. Karlhede, S. A. Kivelson, and E. H. Rezayi, Skyrmions and the crossover from the integer to fractional quantum Hall effect at small Zeeman energies, *Phys. Rev. B* **47**, 16419 (1993).
- [36] J. Sinova, S. M. Girvin, T. Jungwirth, and K. Moon, Skyrmion dynamics and NMR line shapes in quantum Hall ferromagnets, *Phys. Rev. B* **61**, 2749 (2000).
- [37] E. M. Kendirlik, S. Sirt, S. B. Kalkan, W. Dietsche, W. Wegscheider, S. Ludwig, and A. Siddiki, Anomalous resistance overshoot in the integer quantum Hall effect, *Sci. Rep.* **3**, 3133 (2013).
- [38] E. Kendirlik, S. Sirt, S. Kalkan, N. Ofek, V. Umansky, and A. Siddiki, The local nature of incompressibility of quantum Hall effect, *Nat. Commun.* **8**, 14082 (2017).